Electronic Supplementary Information for "Formation and internal ordering of periodic microphases in colloidal models with competing interactions"

Horacio Serna,[1] Antonio Díaz Pozuelo,[2] Eva G. Noya,[2, a)] and Wojciech T. Góźdź[1, b)]
[1)] *Institute of Physical Chemistry Polish Academy of Sciences, Kasprzaka 44/52, 01-224 Warsaw, Poland*
[2)] *Instituto de Química Física Rocasolano, CSIC, C/ Serrano 119, 28006 Madrid, Spain*

(Dated: 26 April 2021)

S1. DETERMINATION OF THRESHOLD VALUE FOR THE BOND ORDER PARAMETER $\bar{q}_{6,limit}$

The fraction of particles within solid-like environments in the lamellar phase was estimated using the averaged bond orientational order parameter proposed by Lechner and Dellago[1]. The appropriate value of the threshold value $\bar{q}_{6,limit}$ to discriminate between solid-like and liquid-like environments was obtained by plotting the distributions of the $\bar{q}_6$ parameter in the liquid-like lamellae and in the solid-like lamellae at $T^* = 0.3$. The effect of temperature on these distributions was investigated by calculating them also at $T^* = 0.2$ for the solid-like lamellae and at $T^* = 0.4$ and $T^* = 0.5$ for the liquid-like lamellae. The distributions were calculated using 100 independent configurations in each case, and taking the cutoff distance $r_c = 1.4\sigma$ to consider two particles as first neighbours. The results are presented in Figure S2. We observe that the distribution of the solid-like lamellae and liquid-like lamellae only overlap over a small range of $\bar{q}_6$. Based on these results, we choose $\bar{q}_{6,limit} = 0.43$ as the threshold value to distinguish solid-like from liquid-like environments.

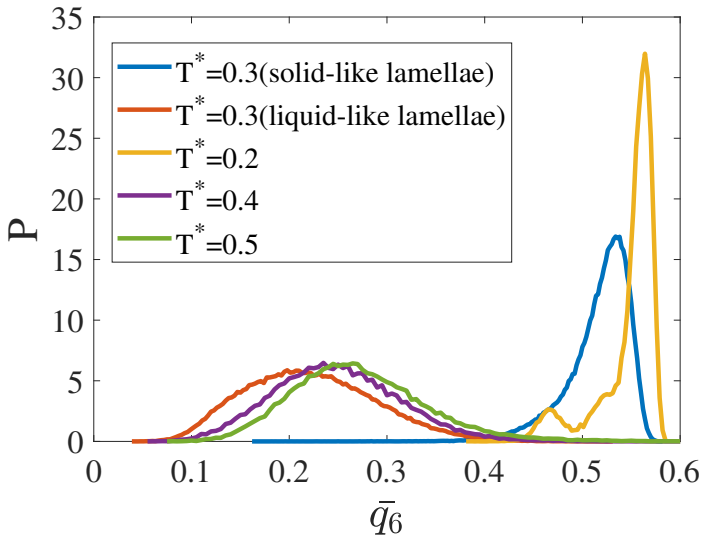

FIG. S1. Probability distributions of the $\bar{q}_6$ parameter at $T^* = 0.3$ for the liquid-like (cooling run) and solid-like (heating run) lamellar phases. The probability distributions at higher (T^* =0.4 and $T^* = 0.5$) and lower ($T^* = 0.2$) temperatures are also plotted. In the calculations of $\bar{q}_6$ we considered that two particles are bonded if the distance between then is lower than 1.4σ, which coincides with the minimum of the PDF in the lamellar phase (see Figure 4 of the manuscript). From this figure, $q_{6,\bar{l}imit} = 0.43$.

With the aim of validating the results obtained with the Lechner and Dellago order parameter, we compared the results with those obtained with the implementation of the order parameter proposed by ten Wolde *et al.*[2,3]. In this latter case, the bond order $q_{6,m}(i)$ $(m = -6, 6)$ is evaluated for each particle i. Then this particle is considered to be

[a)] Electronic mail: eva.noya@iqfr.csic.es
[b)] Electronic mail: wtg@ichf.edu.pl

solid if the dot product of the 13-dimensional vector $q_{6,m}(i)$ and the $q_{6,m}(j)$ vector of a number ξ of nearest neighbours j is above a given threshold d_c. This order parameter needs three parameters: the cutoff distance r_c to consider two particles as first neighbours, the threshold value for the dot product d_c, and ξ. Here we chose $r_c = 1.4\sigma$, $d_c = 0.7$ and $\xi = 6$. As it can be seen in Fig. S2, the results obtained with both order parameters are very similar.

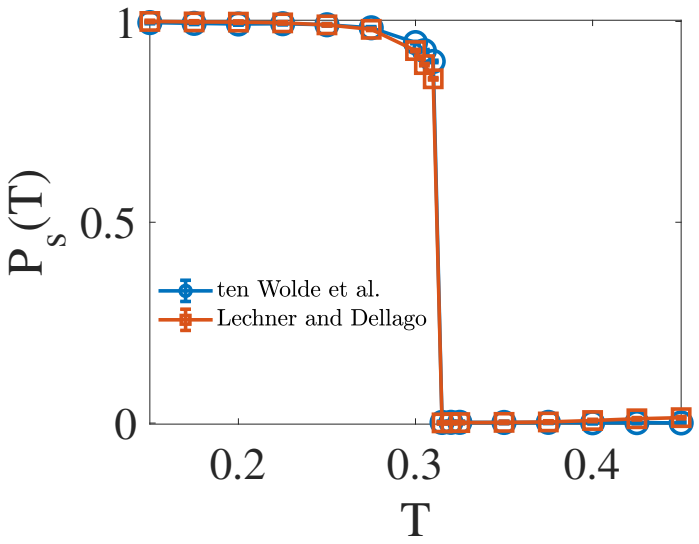

FIG. S2. Comparison of the evolution of particles with solid-like environments in the heating run of the lamellar phase using the Lechner and Dellago[1] order parameter ($\bar{q}_6$) and the one proposed by ten Wolde *et al.*[2,3]

S2. BOND CORRELATION FUNCTION

With the aim of providing further insight into the dynamic behaviour of the periodic microphases we also evaluated the bond correlation function $\phi_B(t)$. This function compares the bonds formed by each particle and its neighbours at a given time t with respect to those at time zero[4]:

$$\phi_B(t) = \frac{\langle \sum_{i<j} n_{ij}(t) n_{ij}(0) \rangle}{N_B(0)} \tag{S1}$$

where the angular brackets denote ensemble average, $n_{ij}(t)$ is a function whose value is one if particles i and j form a bond at time t and zero otherwise. $N_B(0)$ is the number of bonds at time zero.

As can be seen in Fig. S3, the time at which the bond correlation function decreases to half its value increases gradually with temperature in the cluster-crystal and cylindrical phases. In the lamellar phase, the temperature $T^* = 0.30$ falls inside the hysteresis loop observed in the energy and density curves (see Figure 5 in the main text of the article) and, consistently with this, this function behaves differently depending on whether the simulation at $T^* = 0.30$ belongs to a heating or a cooling run (see Figure S3). Considering the results from a heating run, the decay of $\phi_B(t)$ decreases gradually when temperature increases as in the cluster-crystal and cylindrical phases. However, if the simulation at $T^* = 0.30$ is taken from a cooling run, the decay of the correlation time is very pronounced. This is consistent with a situation in which the lamellae are frozen at lower temperatures (which is evidenced by the slow exchange of neighbours of the particles) and that at $T^* \approx 0.30$ undergo a transition to liquid-like lamellae.

Comparing now the evolution of the bond correlation function with density at constant temperature, the particles change bonds at shorter times in the cylindrical phase, followed by the cluster-crystal that exhibits slightly longer decay times, and by the lamellar phase, in which the decay of $\phi_B(t)$ occurs at much longer times, specially at the lower temperatures. Notably, at $T^* = 0.30$, $\phi_B(t)$ decays at shorter times in the lamellar phase than in the cluster-crystal and cylindrical phase if a simulation coming from a cooling run is considered.

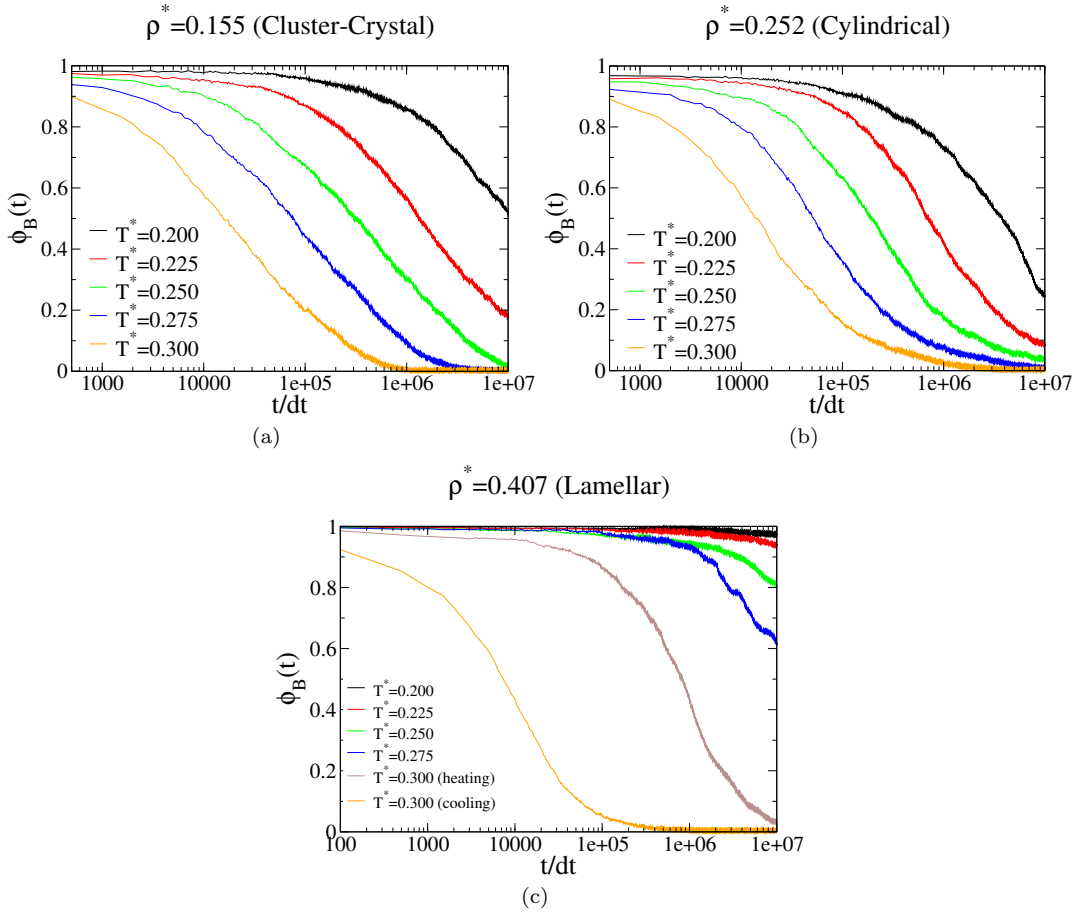

FIG. S3. Bond correlation function for the cluster-crystal, cylindrical and lamellar phases.

S3. CLUSTER-CRYSTAL AT LOW TEMPERATURE

Given the finite size of the spherical clusters formed in the cluster-crystal phase, it is rather straightforward to extract further information about the types of movement contributing to the MSD of the system at the lowest temperatures. First, we measured the number of particles that leave the cluster to which they belong in the initial configuration. As can be seen in Figure S4, at $T^* = 0.200$, after one million MD steps, only a small fraction of particles (about 0.5%) have migrated from one cluster to another, but this proportion increases rapidly at higher temperatures (e.g. at $T^* = 0.225$ about 4% have abandoned their parent cluster after one million MD steps).

Given that at $T^* = 0.200$ the exchange of particles is rather small, it is also relatively easy to measure the MSD using the center of mass of the clusters. As it can be seen in Figure S4, the cluster MSD does not increase at long times, indicating that at this low temperature, long translational moves of the clusters are very unlikely. As can be seen in the movie provided as ESI, the clusters can move due to vibrational and rotational moves about the lattice positions of the cluster-crystal.

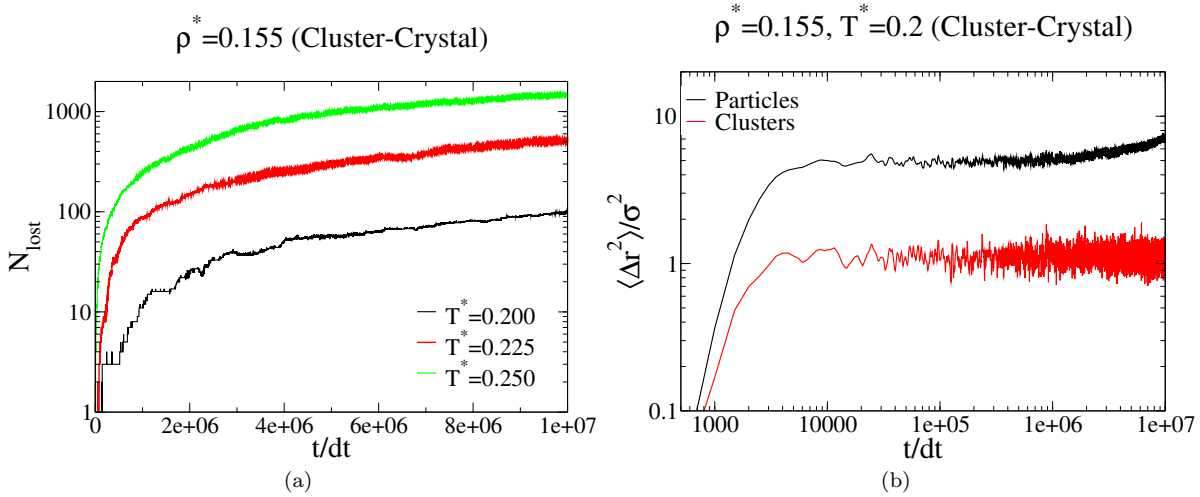

FIG. S4. Analysis of the cluster-crystal phase at low temperature. a) Number of particles that leave the cluster to which they belonged at the beginning of the simulation. b) Mean-squared displacement measured using the particles positions (black line) and the center of mass of the clusters (red line).

S4. SCATTERING FUNCTIONS FITS

We fit the coherent ($F(q,t)$) and incoherent ($F_s(q,t)$) scattering functions obtained from simulations to stretched exponential functions:

$$f(t) = \exp(-(t/\tau)^{\beta}) \tag{S2}$$

Figures S5 and S6 show the fits for $F(q,t)$ and $F_s(q,t)$ respectively. The values of the fit parameters and R^2 are reported in tables S1 and S2 for $F(q,t)$ and $F_s(q,t)$ respectively.

[1]W. Lechner and C. Dellago, J. Chem. Phys. **129**, 114707 (2008).
[2]P.-R. ten Wolde, M. J. Ruiz-Montero, and D. Frenkel, Faraday Discuss. **104**, 93 (1996).
[3]L. Filion, M. Hermes, R. Ni, and M. Dijkstra, J. Chem. Phys. **133**, 244115 (2010).
[4]F. Sciortino, P. Tartaglia, and E. Zaccarelli, J. Phys. Chem. B **109**, 21942 (2005).

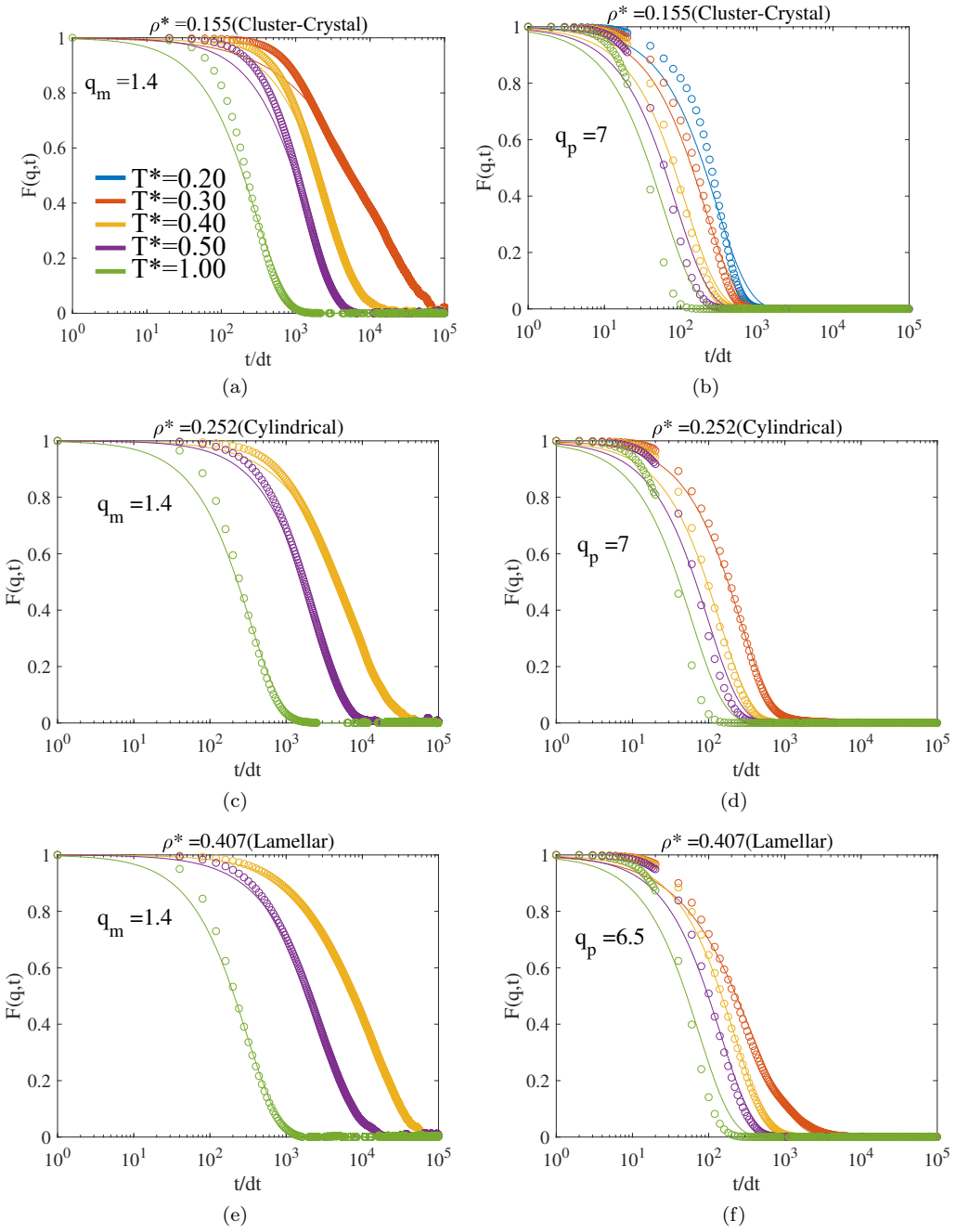

FIG. S5. Coherent scattering functions, $F(q,t)$, for the cluster-crystal, cylindrical and lamellar phases evaluated at the cluster-cluster length scale(q_m) and particle-particle length scale (q_p). The circles are the data from simulations and the solid lines are fits to stretched exponential functions.

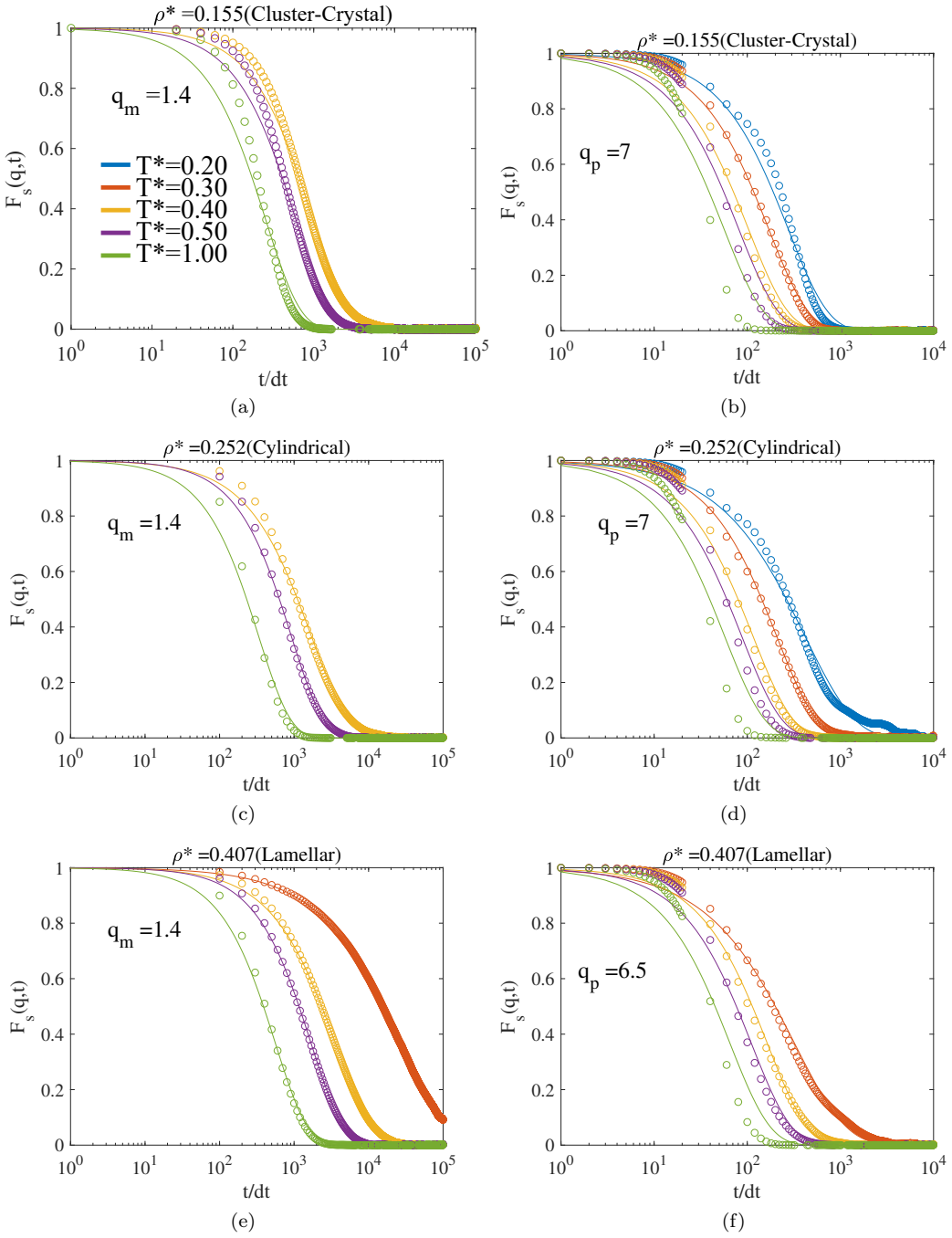

FIG. S6. Incoherent scattering functions, $F_s(q,t)$, for the cluster-crystal, cylindrical and lamellar phases evaluated at the cluster-cluster length scale(q_m) and particle-particle length scale (q_p). The circles are the data from simulations and the solid lines are fits to stretched exponential functions.

TABLE S1. Fit parameters of the coherent scattering function $F(q,t)$.

	$\rho^* = 0.155$ (Cluster-crystal)		$\rho^* = 0.252$ (Cylindrical)		$\rho^* = 0.407$ (Lamellar)	
T^*	q_m	q_p	q_m	q_p	q_m	q_p
0.20	$\tau = --$ $\beta = --$ $R^2 = --$	$\tau = 296.2867$ $\beta = 1.0000$ $R^2 = 0.9916$	$\tau = --$ $\beta = --$ $R^2 = --$	$\tau = --$ $\beta = --$ $R^2 = --$	$\tau = --$ $\beta = --$ $R^2 = --$	$\tau = --$ $\beta = --$ $R^2 = --$
0.30	$\tau = 1.0841 \times 10^4$ $\beta = 0.6636$ $R^2 = 0.9949$	$\tau = 202.9495$ $\beta = 1.0000$ $R^2 = 0.9965$	$\tau = --$ $\beta = --$ $R^2 = --$	$\tau = 257.9252$ $\beta = 1.0000$ $R^2 = 0.9985$	$\tau = --$ $\beta = --$ $R^2 = --$	$\tau = 367.2056$ $\beta = 0.7905$ $R^2 = 0.9958$
0.40	$\tau = 2.8884 \times 10^3$ $\beta = 1.0000$ $R^2 = 0.9957$	$\tau = 118.3306$ $\beta = 1.0000$ $R^2 = 0.9943$	$\tau = 7.3747 \times 10^3$ $\beta = 0.8587$ $R^2 = 0.9966$	$\tau = 136.9300$ $\beta = 1.0000$ $R^2 = 0.9962$	$\tau = 1.2108 \times 10^4$ $\beta = 0.8512$ $R^2 = 0.9963$	$\tau = 214.6687$ $\beta = 1.0000$ $R^2 = 0.9985$
0.50	$\tau = 1.4039 \times 10^3$ $\beta = 1.0000$ $R^2 = 0.9917$	$\tau = 87.8390$ $\beta = 1.0000$ $R^2 = 0.9903$	$\tau = 2.4136 \times 10^3$ $\beta = 1.0000$ $R^2 = 0.9960$	$\tau = 97.5759$ $\beta = 1.0000$ $R^2 = 0.9925$	$\tau = 3.0516 \times 10^3$ $\beta = 0.9116$ $R^2 = 0.9963$	$\tau = 142.1264$ $\beta = 1.0000$ $R^2 = 0.9961$
1.00	$\tau = 3286.4280$ $\beta = 1.0000$ $R^2 = 0.9846$	$\tau = 57.9030$ $\beta = 1.0000$ $R^2 = 0.9830$	$\tau = 331.0405$ $\beta = 1.0000$ $R^2 = 0.9888$	$\tau = 59.2416$ $\beta = 1.0000$ $R^2 = 0.9885$	$\tau = 300.6419$ $\beta = 1.0000$ $R^2 = 0.9915$	$\tau = 74.6857$ $\beta = 1.0000$ $R^2 = 0.9885$

TABLE S2. Fit parameters of the incoherent scattering function $F_s(q,t)$.

	$\rho^* = 0.155$ (Cluster-crystal)		$\rho^* = 0.252$ (Cylindrical)		$\rho^* = 0.407$ (Lamellar)	
T^*	q_m	q_p	q_m	q_p	q_m	q_p
0.20	$\tau = --$ $\beta = --$ $R^2 = --$	$\tau = 274.1604$ $\beta = 1.0000$ $R^2 = 0.9953$	$\tau = --$ $\beta = --$ $R^2 = --$	$\tau = 415.1450$ $\beta = 0.8058$ $R^2 = 0.9896$	$\tau = --$ $\beta = --$ $R^2 = --$	$\tau = --$ $\beta = --$ $R^2 = --$
0.30	$\tau = --$ $\beta = --$ $R^2 = --$	$\tau = 169.4021$ $\beta = 1.0000$ $R^2 = 0.9982$	$\tau = --$ $\beta = --$ $R^2 = --$	$\tau = 206.2207$ $\beta = 1.0000$ $R^2 = 0.9989$	$\tau = 2.6564 \times 10^4$ $\beta = 0.6790$ $R^2 = 0.9998$	$\tau = 320.4111$ $\beta = 0.7797$ $R^2 = 0.9958$
0.40	$\tau = 965.3414$ $\beta = 1.0000$ $R^2 = 0.9956$	$\tau = 102.6534$ $\beta = 1.0000$ $R^2 = 0.9938$	$\tau = 1.7007 \times 10^3$ $\beta = 0.8610$ $R^2 = 0.9961$	$\tau = 114.8576$ $\beta = 1.0000$ $R^2 = 0.9960$	$\tau = 3.5903 \times 10^3$ $\beta = 0.8603$ $R^2 = 0.9994$	$\tau = 163.6459$ $\beta = 1.0000$ $R^2 = 0.9983$
0.50	$\tau = 595.5857$ $\beta = 1.0000$ $R^2 = 0.9941$	$\tau = 80.6905$ $\beta = 1.0000$ $R^2 = 0.9894$	$\tau = 916.5354$ $\beta = 1.0000$ $R^2 = 0.9981$	$\tau = 86.9110$ $\beta = 1.0000$ $R^2 = 0.9919$	$\tau = 1.6872 \times 10^3$ $\beta = 0.9896$ $R^2 = 0.9996$	$\tau = 110.3181$ $\beta = 1.0000$ $R^2 = 0.9957$
1.00	$\tau = 251.8659$ $\beta = 1.0000$ $R^2 = 0.9783$	$\tau = 56.1555$ $\beta = 1.0000$ $R^2 = 0.9830$	$\tau = 333.4213$ $\beta = 1.0000$ $R^2 = 0.9875$	$\tau = 56.9122$ $\beta = 1.0000$ $R^2 = 0.9852$	$\tau = 559.6968$ $\beta = 1.0000$ $R^2 = 0.9961$	$\tau = 65.0518$ $\beta = 1.0000$ $R^2 = 0.9878$